Cell, Volume *134*

Supplemental Data

Identification of a Lipokine,

a Lipid Hormone Linking Adipose Tissue

to Systemic Metabolism

Haiming Cao, Kristin Gerhold, Jared R. Mayers, Michelle M. Wiest, Steven M. Watkins, and Gökhan S. Hotamisligil

Supplemental Experimental Procedures

Bioinformatics and statistical analysis

Multivariate analyses were used to examine trends over entire lipid profiles. Data were first cleaned by removing analytical outliers and poorly measured metabolites (those with more than 30% of observations below the limit of detection). Next, to ensure that variables being entered into the multivariate analyses are relevant to the experimental groups, a one-way ANOVA over all groups was conducted, and only those metabolites reaching a p-value of 0.05 or below are included. Using only those metabolites which reached a p-value of 0.05 or below in the one-way ANOVA, hierarchical clustering was used to evaluate where the largest differences existed in the lipid profiles. The lower on the tree the branch is, the more similar the group, alternatively, the higher the branch, the more disparate the groups. We further examined the entire profiles using principle component analysis (PCA). PCA is a way to explain the variance-covariance structure of a set of variables through a few linear combinations of those variables; each linear combination is called a principal component. In most cases, however, the variance can be described by a small number of principle components. Scatter plots of the first and second principal components were used to illustrate how they discriminated the treatment groups.

Given the results of the first two multivariate analyses, we devised another way of examining the effects. This approach compares the diet effect in the $FABP^{-/-}$ mice to the diet effect in the wild type (WT) mice for each tissue. We calculated the strength of difference (by p-values) in the diet in the WT and $FABP^{-/-}$ mice over all fatty acids in all lipid classes. Then we plotted the ranked p-values of the $FABP^{-/-}$ against those of the WT. Each point on a line indicates the number of p-values of one group that are smaller than the p-value of equal ranking of the other group. For instance, in liver, the first five ranked p-values of the comparison between diets in the WT mice were smaller than the first five ranked p-values of the same comparison in KO mice (thus, the x-intercept of the liver line is (0,5)).

If the magnitude of the effects of diet on the total lipid profiles on the WT and $FABP^{-/-}$ mice were approximately the same, the line would follow the y=x line. A line above the y=x would indicate a stronger effect in the $FABP^{-/-}$ mice, where a line below the y=x axis would indicate a stronger effect in the WT mice.

Breaking down the entire lipid profile into lipid classes, we used heat maps to investigate changes in fatty acid composition induced by treatment for each lipid class. Using results of the one-way ANOVA performed on each metabolite, significance was evaluated by comparing the F-statistic of the observed data to the distribution of the F-statistic obtained from randomly permuted data. The F-statistic of the observed data was displayed as red diamonds over the distribution of F-statistics from the permuted data. The heat map displays the observed data, centered to the mean of the placebo group and scaled by the standard deviation of all observations. This graphic was used to determine the magnitude of the effect in a lipid class and identify which fatty acids were changed in that lipid class.

Cell culture, fatty acid treatment, glucose uptake and reporter assays

FAO rat hepatocytes were maintained in 10% FBS. For lipid treatment experiments, FAO cells infected with reporter adenoviruses were treated in 2% fatty acid-free BSA overnight and FAO cells expressing Flag-tagged SCD-1 were treated for 4 hrs. Luciferase assays were performed with dual-glow luciferase system (Promega Corporation) and all values are Firefly normalized to Renilla luciferase activities. C2C12 myoblasts were plated in 96 wells plates coated with 0.2% and differentiated in 2% horse serum upon confluence. Four days post differentiation, C2C12 myotubes were treated overnight with serum-free medium with 2% fatty acid-free BSA and lipids extracted from plasma of WT or FABP$^{-/-}$ mice. Cells were then treated with 100 nM insulin for 10 mins and proteins extracted to analyze with a phospho-Akt ELISA system (R&D Systems, Inc) based on the manufacturer's recommendations. Results were normalized to total protein amount in each well. Glucose uptake in myotubes were performed as previously described (Somwar et al., 2001). MCP1 levels in fat explants treated with plasma lipids were determined with a MCP1 ELISA system (R&D Systems, Inc).

Construction of expression and luciferase reporter adenoviruses

Expression adenoviruses were constructed by cloning aP2, mal1, and SCD-1 cDNAs in adenovirus vector pAD/CMV/V5-DEST and viruses were produced as described in Virapower Adenovirus System (Invitrogen Life Technologies). SCD-1 (-1500 bp) or FAS (-700 bp) promoters were amplified from mouse genomic DNA with PCR and cloned upstream of Firefly luciferase gene of vector pGL3 (Promega Corporation). The mutant SCD-1 promoter was produced by inserting two partial fragments of the -1500 bp promoter lacking the 60bp PUF element in front of luciferase gene in vector pGL3. The entire reporter cassettes were cloned into vector pAD/PL-DEST (Invitrogen Life Technologies) to produce adenoviruses.

Adipocyte and stromal vascular fractionation

Epidydamal fat pads were dissected and transfered into a 50 ml conical tube containing 9 ml of 2% BSA in Krebs-Ringer bicarbonate/hepes (KRBH) buffer and then chopped into small pieces. One ml of freshly prepared collagenase II (10mg/ml, Sigma C6885) was added and incubated at 37 °C for 20 mins with continuous shaking. After tissues were fully digested, cell suspensions were diluted with 15 ml of 2% BSA/KRBH and filtered through 250 mm nylon mesh. Cell filtrates were centrifuged at 600 rpm for 3 min at RT. The floating adipocytes were transferred into new tubes and 10ml of 5 mM EDTA in 2% BSA/PBS was added to the cells to help dissociation of immune cells from adipocytes.•• Adipocyte suspensions were centrifuged at 1,000 rpm (200 x g) for 1 min at RT.•• Floating adipocyte fractions were carefully transfered into 6-well plates. The

original culture tubes were spun down again at 1700 rpms for 10 min to collect the SV fraction and the cells plated in 6-well plates.

Pre-adipocyte cell line production

Pre-adipocyte cell lines were established using the 3T3 protocol (Todaro and Green, 1963) from WT and FABP-deficient mice. Briefly, primary mouse embryo fibroblasts were continuously cultured and transferred every 3 days. The cells' growth rate was initially declined and recovered to a level at the beginning. These cultures were considered established lines. WT and FABP$^{-/-}$ pre-adipocytes differentiated into mature adipocytes equivalently in 6 to 8 days using a standard differentiation protocol (Figure S12).

RNA extraction and quantitative real-time PCR analysis

Total RNA was isolated from liver tissues using Trizol reagent (Invitrogen). Reverse transcription was carried out with superscript first-strand cDNA synthesis system (Applied Biosystems Inc.) using 1 μg of RNA. Quantitative, real-time RT-PCR was performed on a PCR thermal cycler (Applied Biosystems Inc.) The PCR program was: 2 min 30 s at 95°C for enzyme activation, 40 cycles of 15 s at 95°C, 30 s at 58°C, and 1 min at 72°C for extension. Melting curve analysis was performed to confirm the real-time PCR products. All quantitations were normalized to the 18S rRNA or beta-actin levels as indicated. Primer sequences used are provided in the supplemental materials (Figure S15).

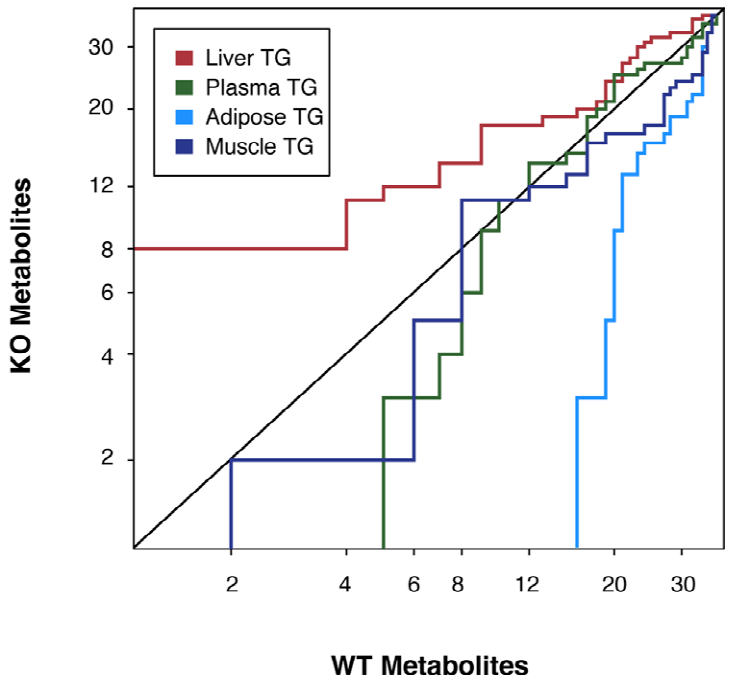

Figure S1. Quantification of dietary effect on tissue triglyceride (TG) metabolism. Strength of differences between diets in the WT and FABP$^{-/-}$ (KO) mice over all fatty acids in triglycerides. The line plot is the ranked p-values of the KO against those of the WT in each tissue.

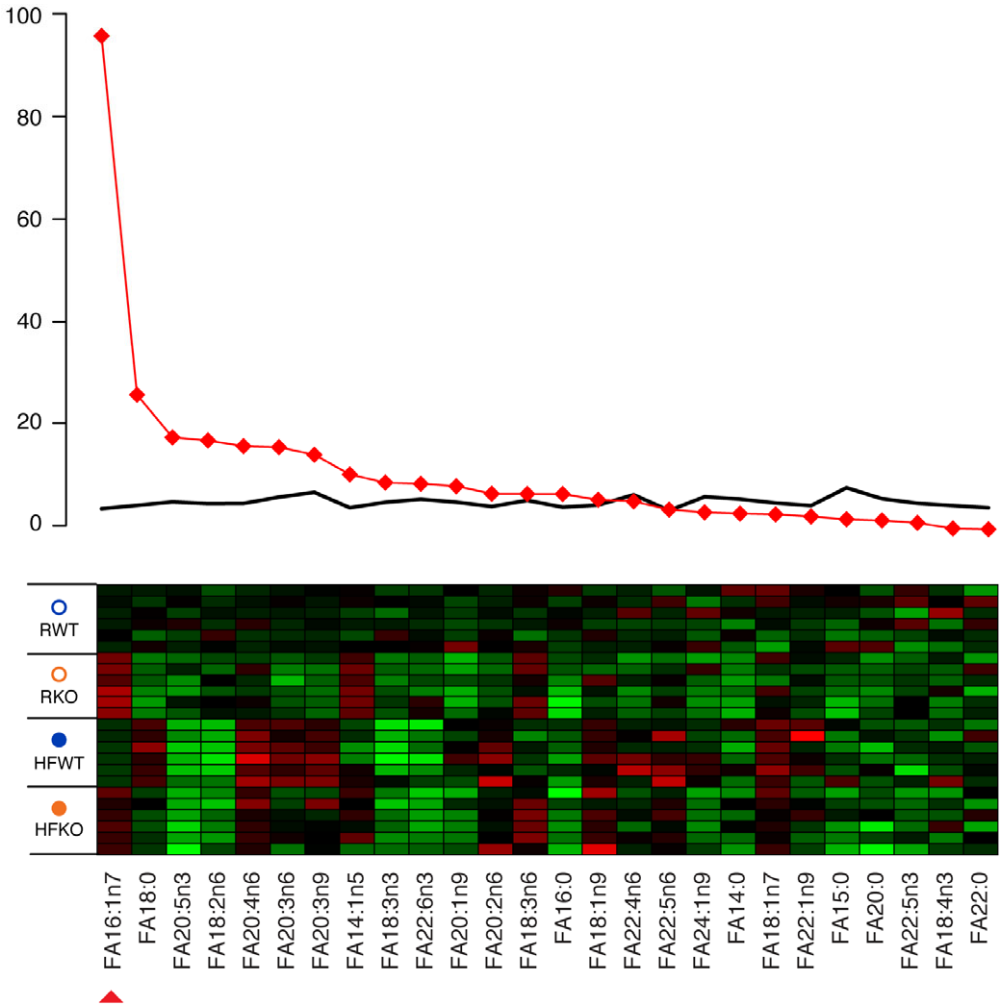

Figure S2. Lipid class composition analysis of plasma free fatty acids of WT or FABP$^{-/-}$ mice.

The F-statistics from a one-way ANOVA are displayed as red diamonds over the distribution of F-statistics from permuted data. The heat map displays the observed data, centered to the mean of the control group and scaled by the standard deviation of all observations.

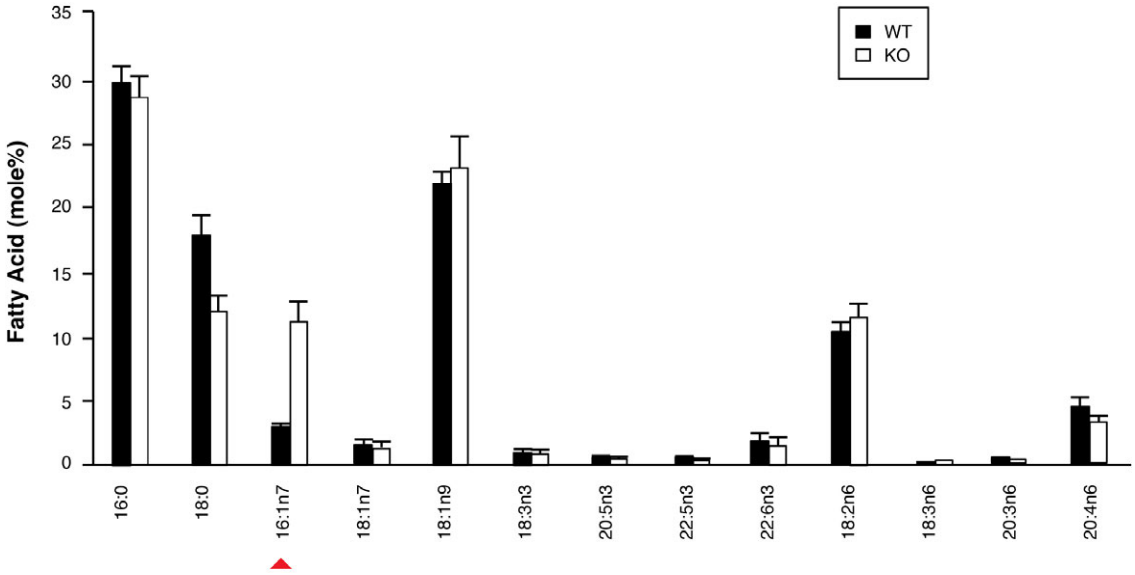

Figure S3. Plasma fatty acid profiles of WT and FABP$^{-/-}$ mice on HFD.
Plasma free fatty acids of WT and FABP$^{-/-}$ mice on HFD were determined as described in Experimental Procedures and expressed as in Figure 2C. Error bars represent SEM.

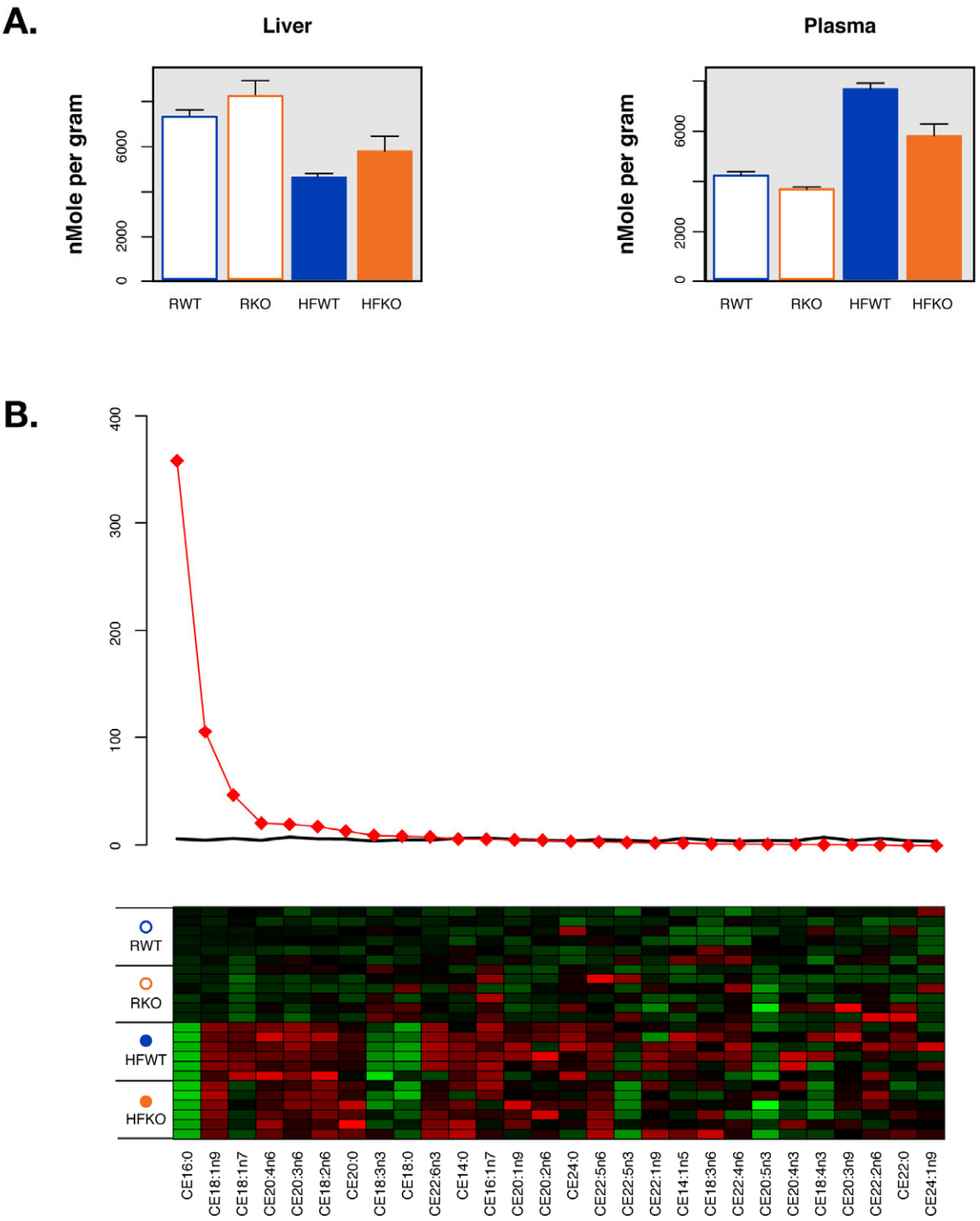

Figure S4. Cholesterol ester metabolism in WT and FABP$^{-/-}$ mice.
A. Cholesterol ester levels in liver and plasma of WT and FABP$^{-/-}$ mice. Error bars represent SEM. **B.** Fatty acid composition analysis for cholesterol ester in liver. The F-statistics from a one-way ANOVA are displayed as red diamonds over the distribution of F-statistics from permuted data. The heat map displays the observed data, centered to the mean of the control group and scaled by the standard deviation of all observations.

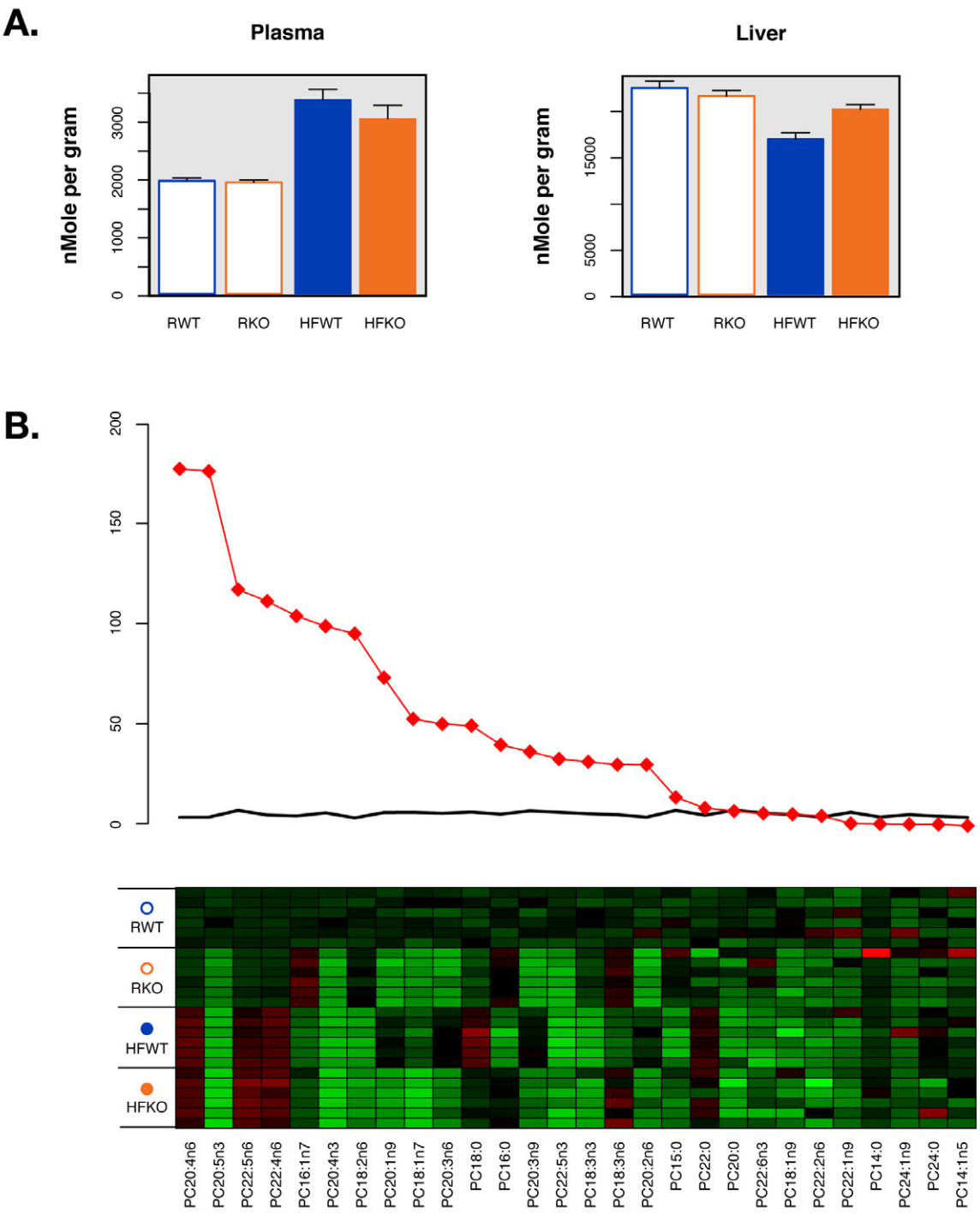

Figure S5. Phosphatidylcholine metabolism in WT and FABP$^{-/-}$ mice.
A. Phosphatidylcholine levels in liver and plasma of WT and FABP$^{-/-}$ mice. Error bars represent SEM. **B.** Fatty acid composition analysis for phosphatidylcholine in liver. The F-statistics from a one-way ANOVA are displayed as red diamonds over the distribution of F-statistics from permuted data. The heat map displays the observed data, centered to the mean of the control group and scaled by the standard deviation of all observations.

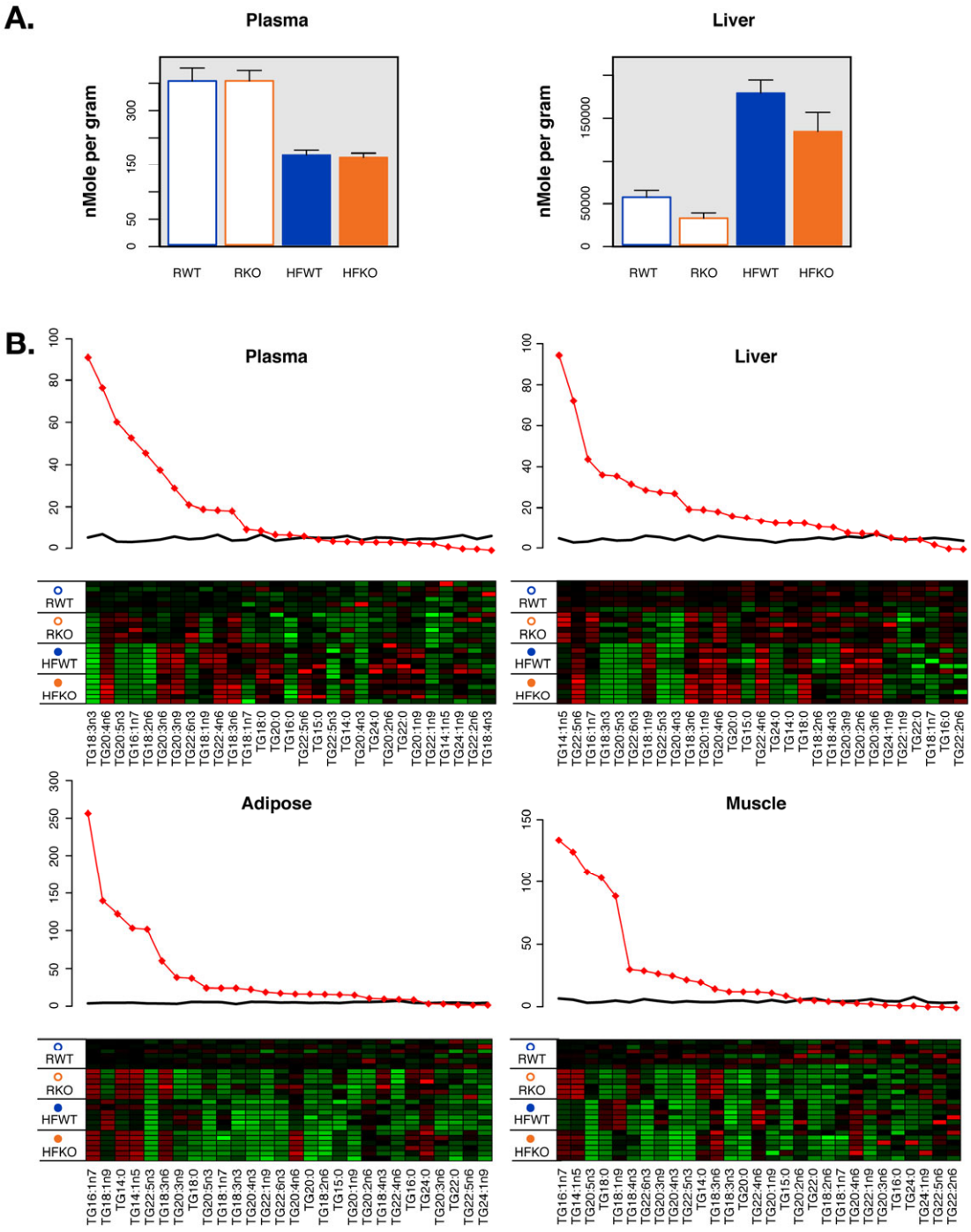

Figure S6. Triglyceride metabolism in WT and FABP$^{-/-}$ mice.
A. Triglyceride levels in liver and plasma WT and FABP$^{-/-}$ mice. Error bars represent SEM. **B.** Fatty acid composition analysis for triglyceride in plasma, liver, muscle, adipose tissue. The F-statistics from a one-way ANOVA are displayed as red diamonds over the distribution of F-statistics from permuted data. The heat map displays the observed data, centered to the mean of the control group and scaled by the standard deviation of all observations.

	Mean				P-value	
	HKO	**HWT**	**RKO**	**RWT**	**RKO vs HKO**	**RWT vs HWT**
DG16:1n7	16.15	3.86	18.84	6.03	0.01	0.02
FA16:1n7	11.10	5.73	13.92	6.26	0.20	0.79
PC16:1n7	4.43	2.92	5.07	2.38	0.53	0.60
TG16:1n7	18.07	3.49	18.17	5.64	0.87	0.00

Figure S7. **Palmitoleate in adipose tissue of WT or FABP$^{-/-}$ mice under either regular or high-fat diets.**
The differences among groups were calculated using Post-hoc comparisons to specifically capture the pairwise effects of HFD on WT or FABP$^{-/-}$ mice.

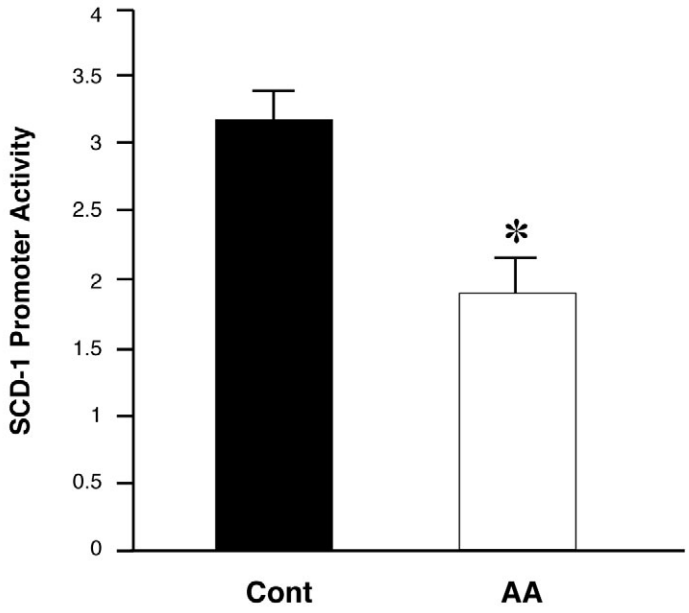

Figure S8. Regulation of SCD-1 promoter activity by PUFA in hepatocytes.
FAO hepatocytes were infected with SCD-1 promoter reporter-carrying adenoviruses and treated with arachidonic acid (AA) at 300 μM overnight. Promoter activity was determined by measuring luciferase activity. Error bars represent SEM.

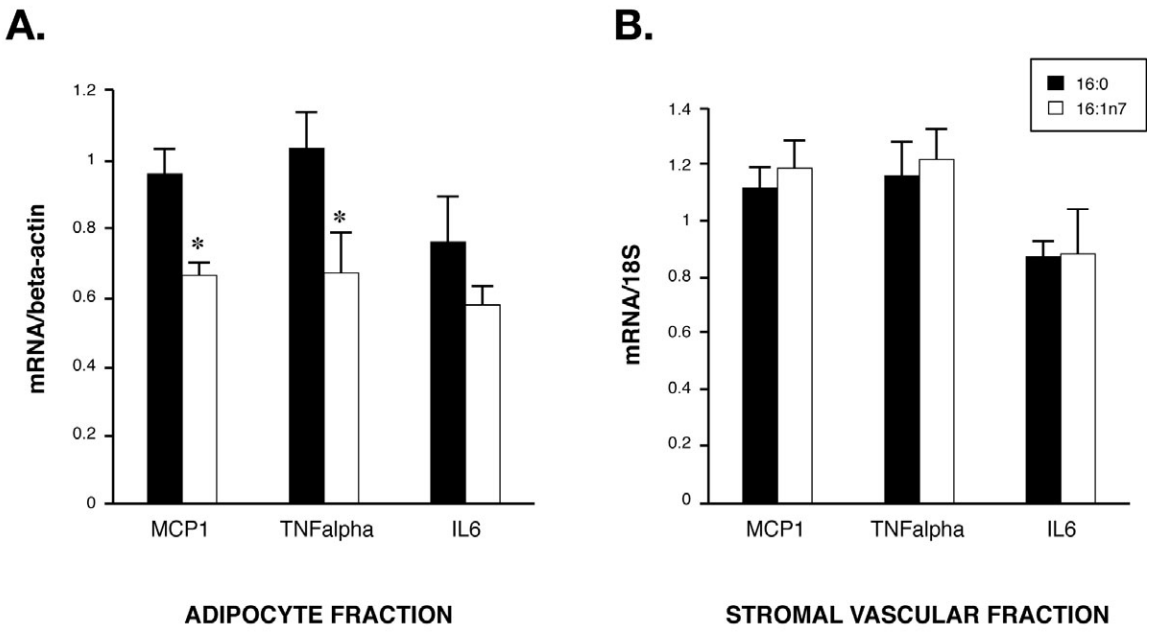

Figure S9. Cytokine expression in adipocyte and stromal vascular fractions treated with fatty acids.

Epidydamal fat pads were dissected from WT mice and separated into adioycte and stromal vascular fractions as described in Experimental Procedures. Each fraction was treated with palmitate or palmitoleate at 500 μM for 2 hrs. Gene expression was determined with quantitative real-time PCR. Error bars represent SEM. **A.** MCP1, TNFalpha and IL6 expression in adipose fraction. **B.** MCP1, TNFalpha and IL6 expression in stromal vascular fraction.

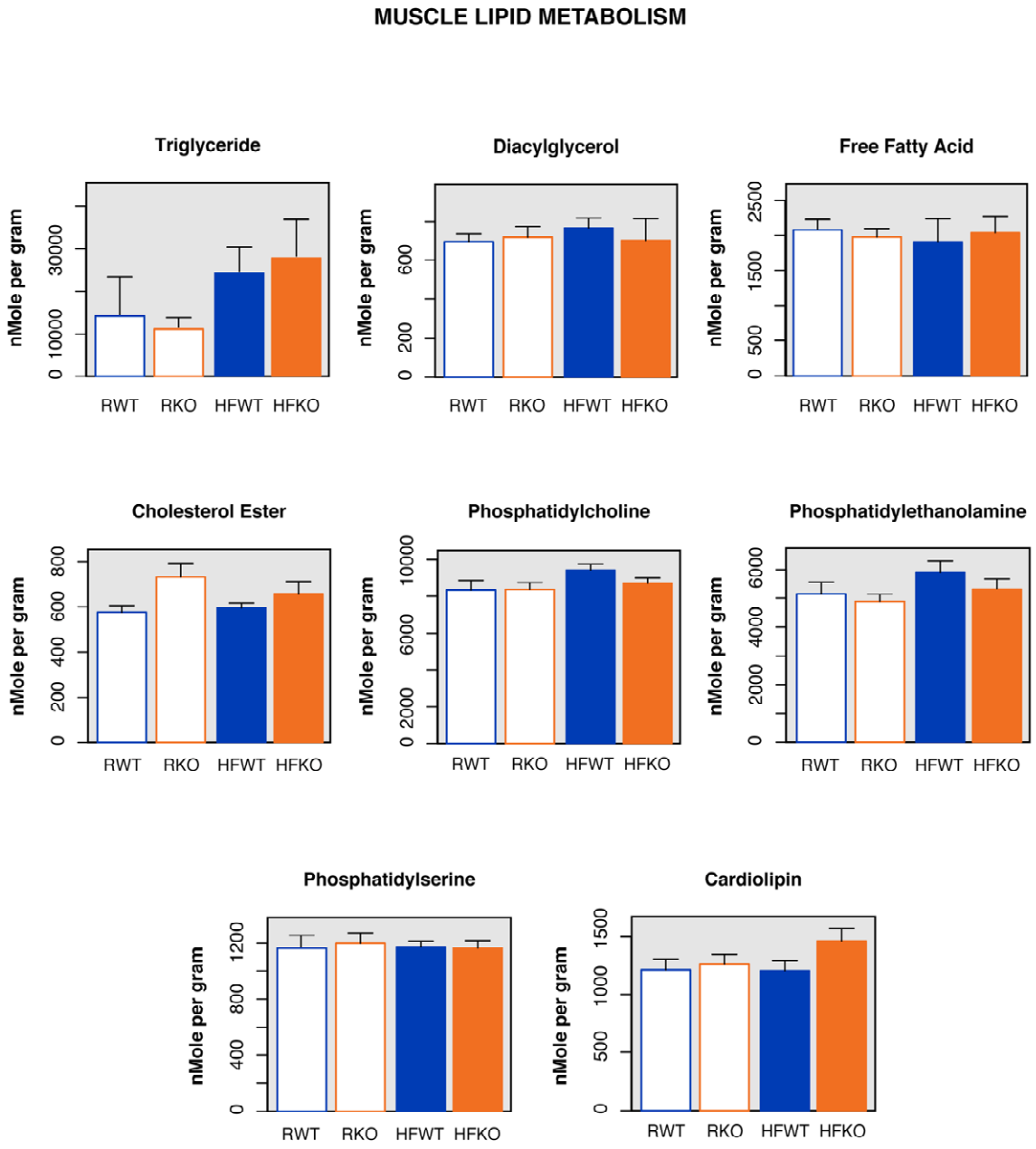

Figure S10. Lipid metabolism in muscle tissue of WT or FABP$^{-/-}$ mice.
Lipids from muscle of WT or FABP$^{-/-}$ mice were quantified as described in Experimental Procedures and expressed as nmol per gram. Error bars represent SEM.

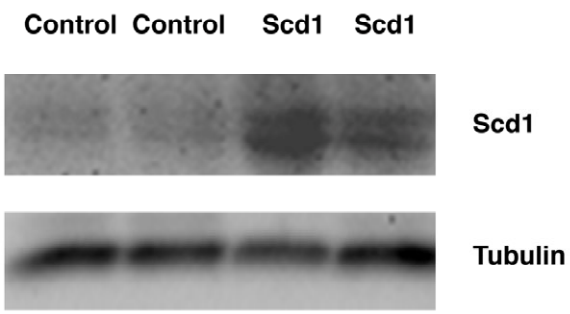

Figure S11. Adenovirus-mediated expression of SCD-1 in liver tissue of FABP$^{-/-}$ mice.
FABP$^{-/-}$ mice maintained on HFD were injected with control or SCD-1 adenoviruses. SCD-1 protein levels in liver tissues were determined with immunoblotting. Tubulin was used as a loading control.

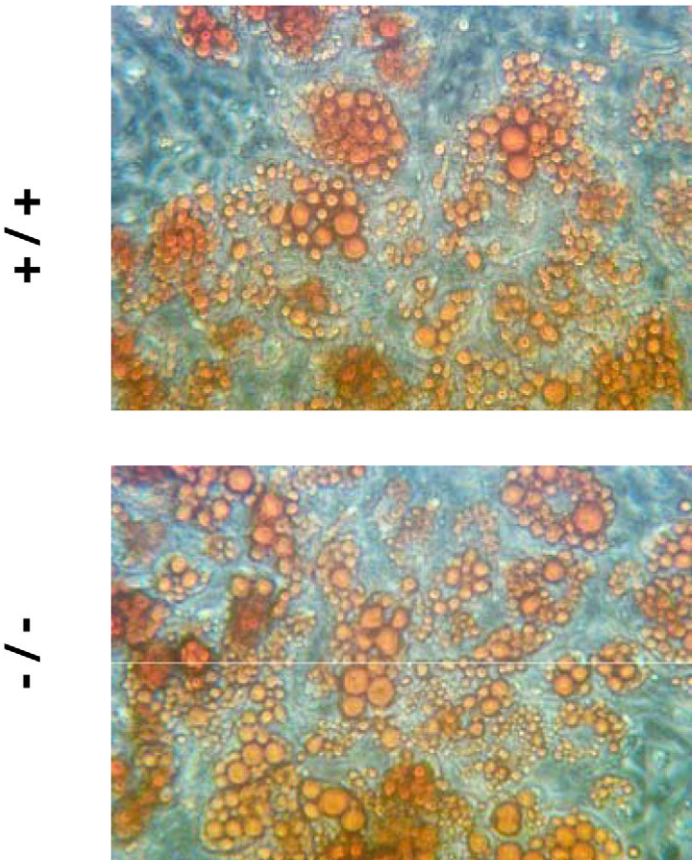

Figure S12. Images of differentiated WT and FABP$^{-/-}$ adipocytes.
Pre-adipocyte cell lines were derived from WT (+/+) or FABP-deficient (-/-) mice as described in Experimental Procedures and differentiated into mature adipocytes. Cells were fixed and stained with Oil-red-O.

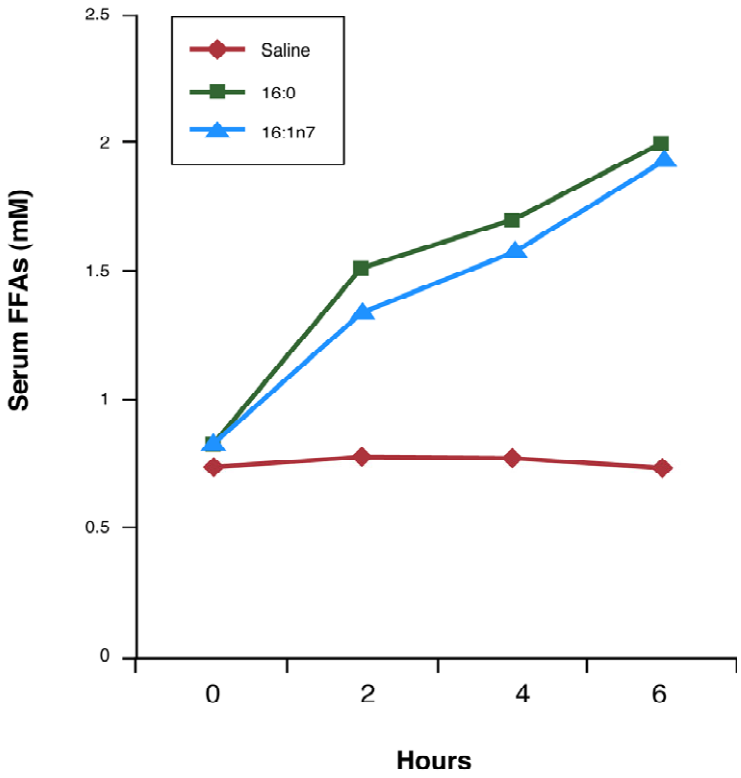

Figure S13. Plasma fatty acid levels during lipid-infusion.
Blood was collected by tail bleeding from mice that were infused with either TG-palmitate (16:0) or TG-palmitoleate (16:1n7) and plasma free fatty acids were determined with a fatty acid assay kit as described in Experimental Procedures.

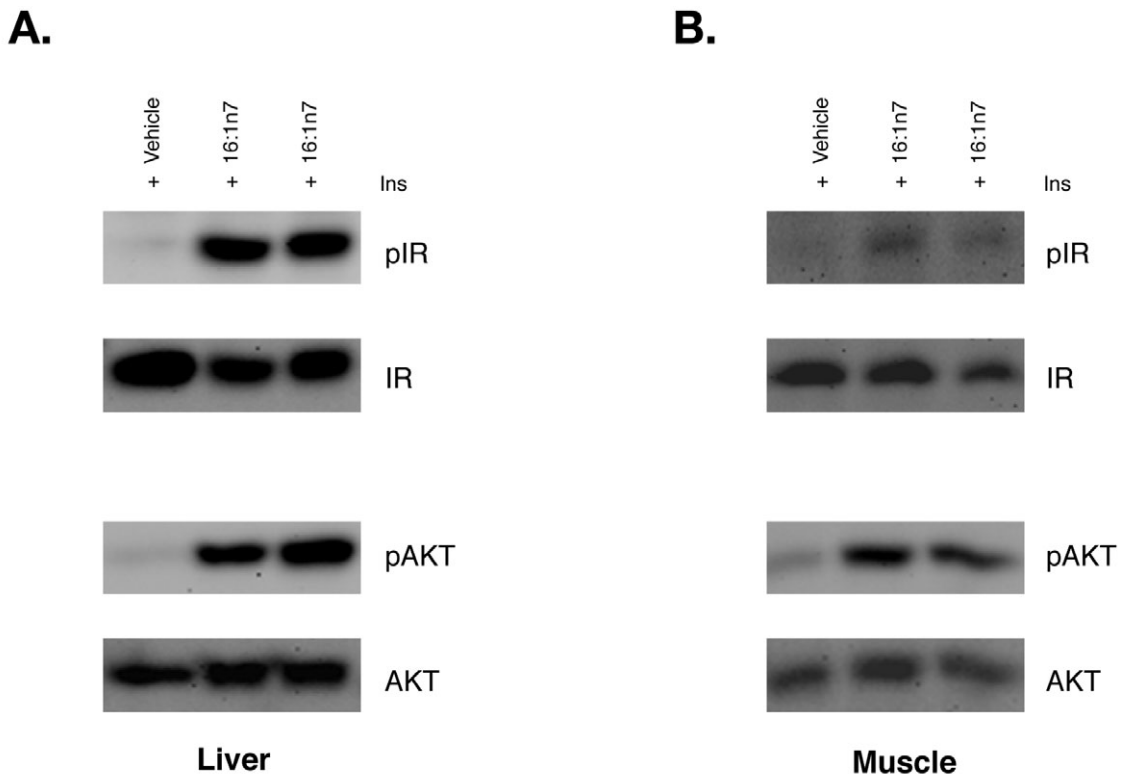

Figure S14. Insulin signaling in mice infused with vehicle or palmitoleate.
A. Insulin-stimulated phosphorylation of insulin receptor and AKT in liver of mice infused with vehicle or palmitoleate**. B.** Insulin-stimulated phosphorylation of insulin receptor and AKT in muscle of mice infused with vehicle or palmitoleate**.** Mice were infused with vehicle or palmitoleate at 3.3 μl/min for 6 hrs and insulin (1U/Kg) was injected through the infusing tubing. Three minutes after insulin injection, tissues were collected and immunobloting analyses were performed.

PRIMER SEQUENCES FOR QUANTITATIVE REAL-TIME PCR

18s
Forward Primer AGTCCCTGCCCTTTGTACACA
Reverse Primer CGATCCGAGGGCCTCACTA

Beta-actin
Forward Primer GCTGTGCTATGTTGCTCTA
Reverse Primer CGCTCGTTGCCAATAGTG

ACC1
Forward Primer CTTCCTGACAAACGAGTCTGG
Reverse Primer CTGCCGAAACATCTCTGGGA

FAS
Forward Primer GGAGGTGGTGATAGCCGGTAT
Reverse Primer TGGGTAATCCATAGAGCCCAG

SCD-1
Forward Primer TTCTTGCGATACACTCTGGTGC
Reverse Primer CGGGATTGAATGTTCTTGTCGT

ELOVL6
Forward Primer GAAAAGCAGTTCAACGAGAACG
Reverse Primer AGATGCCGACCACCAAAGATA

SPOT 14
Forward Primer ATGCAAGTGCTAACGAAACGC
Reverse Primer CCTGCCATTCCTCCCTTGG

DGAT1
Forward Primer TCCGTCCAGGGTGGTAGT
Reverse Primer TGAACAAAGAATCTTGCAGACGA

Figure S15. Primer sequences for quantitative real-time PCR.

Supplemental References

Somwar, R., Niu, W., Kim, D. Y., Sweeney, G., Randhawa, V. K., Huang, C., Ramlal, T., and Klip, A. (2001). Differential effects of phosphatidylinositol 3-kinase inhibition on intracellular signals regulating GLUT4 translocation and glucose transport. J Biol Chem *276*, 46079-46087.

Todaro, G. J., and Green, H. (1963). Quantitative studies of the growth of mouse embryo cells in culture and their development into established lines. J Cell Biol *17*, 299-313.